Adhesive Coatings

Deutsche Ausgabe: DOI: 10.1002/ange.201510319
Internationale Ausgabe: DOI: 10.1002/anie.201510319

Nanomechanics of Poly(catecholamine) Coatings in Aqueous Solutions

Chanoong Lim[+], Jun Huang[+], Sunjin Kim[+], Haeshin Lee, Hongbo Zeng,* and Dong Soo Hwang**

Abstract: *Mussel-inspired self-polymerized catecholamine coatings have been widely utilized as a versatile coating strategy that can be applied to a variety of substrates. For the first time, nanomechanical measurements and an evaluation of the contribution of primary amine groups to poly(catecholamine) coatings have been conducted using a surface-forces apparatus. The adhesive strength between the poly(catecholamine) layers is 30-times higher than that of a poly(catechol) coating. The origin of the strong attraction between the poly(catecholamine) layers is probably due to surface salt displacement by the primary amine, π–π stacking (the quadrupole–quadrupole interaction of indolic crosslinks), and cation–π interactions (the monopole–quadrupole interaction between positively charged amine groups and the indolic crosslinks). The contribution of the primary amine group to the catecholamine coating is vital for the design and development of mussel-inspired catechol-based coating materials.*

Mussels secrete protein-based adhesive materials that facilitate the attachment of mussels to a variety of substrates in marine environments, which are characterized by salinity and turbulence. This strong and water-resistant adhesion is particularly useful for biotechnological and medical applications, such as tissue engineering in the human body, where water is ubiquitous. Mussel adhesive proteins have, in particular, drawn significant attention. Waite and Tanzer reported that 3,4-dihydroxy-L-phenylalanine (DOPA), the catecholic unusual amino acid formed by post-translational modifications of tyrosine, is primarily responsible for the adhesive function in aqueous environments.[1] Subsequently, various catechol-containing polymers with adhesive properties, such as poly(ethylene glycol)-catechols,[2] chitosan-catechol,[3] and alginate-catechol,[4] were prepared. However, none of these exhibited material-chemistry-independent surface attachment, a property unique to marine mussels. The key factor that helps achieve material-independent adhesion is the presence of basic amino acids, lysine,[5] and histidine,[6] adjacent to DOPA with a similar stoichiometric ratio between lysine and DOPA (i.e., DOPA: ca. 20 %, lysine ca. 20 % in the amino acid composition of mfp-1). Dopamine, a mussel-inspired building block that exploits the above-mentioned adhesive chemistry of DOPA and lysine/histidine, is the first molecule to exhibit material-independent surface coating via its oxidative polymerization (i.e., formation of poly-(dopamine)).[5a] The practical utility of poly(dopamine) in the field of surface chemistry has led to it rapidly becoming an emerging tool for controlling surface properties in applications, such as mammalian cell attachment,[7] stem cell growth,[8] depots for drug delivery,[9] biosensors, energy-storage devices such as Li-ion,[4b,10] Li-air,[11] and Li-S batteries, [12] and microfluidic devices.[13]

The adhesion mechanism of a catechol moiety, which is the side chain of DOPA, was studied by measurements of its binding force at a single-molecule level using an atomic force microscope (AFM).[14] The study revealed that the catechol reversibly binds to oxide surfaces by a coordination mechanism with a force magnitude between 0.7 and 0.8 nN, which increases up to 2 nN when interacting with organic surfaces by breaking a covalent bond. Furthermore, the adhesion force of mussel foot proteins to various substrates was investigated using a surface-forces apparatus (SFA).[15] Despite the importance of amines in material-independent surface chemistry, investigating the adhesion force of catechol and amine at an interface remains a challenge. Poly(dopamine) is a candidate polymer for use in this purpose, but the formation of rough interfaces after coating renders this an unsuitable platform for nano-mechanical techniques, such as SFA or AFM, which generally require surface smoothness at the nanoscale. When 3,4-dihydroxyindole (DHI), a critical intermediate in poly(dopamine) coating, is polymerized, two distinct morphologies in the form of nanospheres and nanosheets co-exist on the surfaces. In fact, methods for preparing poly(dopamine) nanoparticles utilize the intrinsic nature of the oxidative polymerization of DHI to give spherical particles.[16] Chemical derivatives of poly(dopamine) with a sustained capacity for material-independent surface chemistry have been reported.[17] Among these, the poly(norepinephrine) (pNE) coating results in atomically smooth surfaces,[18] which provides a suitable platform for the aforementioned nanomechanical measurements.

---

[*] C. Lim,[+] Prof. D. S. Hwang
School of Interdisciplinary Bioscience and Bioengineering, Division of Integrative Biosciences and Biotechnology, School of Environmental Science and Engineering, Pohang University of Science and Technology (POSTECH)
Pohang 790-784 (Korea)
E-mail: dshwang@postech.ac.kr

J. Huang,[+] Prof. H. Zeng
Department of Chemical and Materials Engineering
University of Alberta
Edmonton, Alberta, T6G 2V4 (Canada)
E-mail: hongbo.zeng@ualberta.ca

S. Kim,[+] Prof. H. Lee
Department of Chemistry, Graduate School of Nanoscience and Technology (WCU) and KAIST institute NanoCentury, Korea Advanced Institute of Science and Technology
Daejeon 305-701 (Korea)
E-mail: haeshin@kaist.ac.kr

[+] These authors contributed equally to this work.

Supporting information and the ORCID identification number(s) for the author(s) of this article can be found under http://dx.doi.org/10.1002/anie.201510319.

Herein, we report direct evidence regarding the interfacial contributions of a primary amine group to material-independent surface chemistry by utilizing pNE as a model system. Norepinephrine (NE) is one of the catecholamine neurotransmitters with a structure similar to dopamine (Scheme 1). The smooth coated surface of pNE makes it suitable for the measurement of the interaction forces of catechol and amine. Therefore, by utilizing NE, we can explicate the rationale behind primary amines playing a key role in the strong adhesion of catechol-based materials. As a control, the interaction of poly(pyrocatechol) (pPC), a self-polymerized catechol without any amine moiety, was also tested using SFA. Recently, polyphenols such as tannic acid[19] have been used in the surface functionalization of a wide variety of materials. However, our data suggest that the contribution from the primary amine groups or assistance from metal ions or metal oxides should not be overlooked when attempting to coat a surface evenly and thickly.

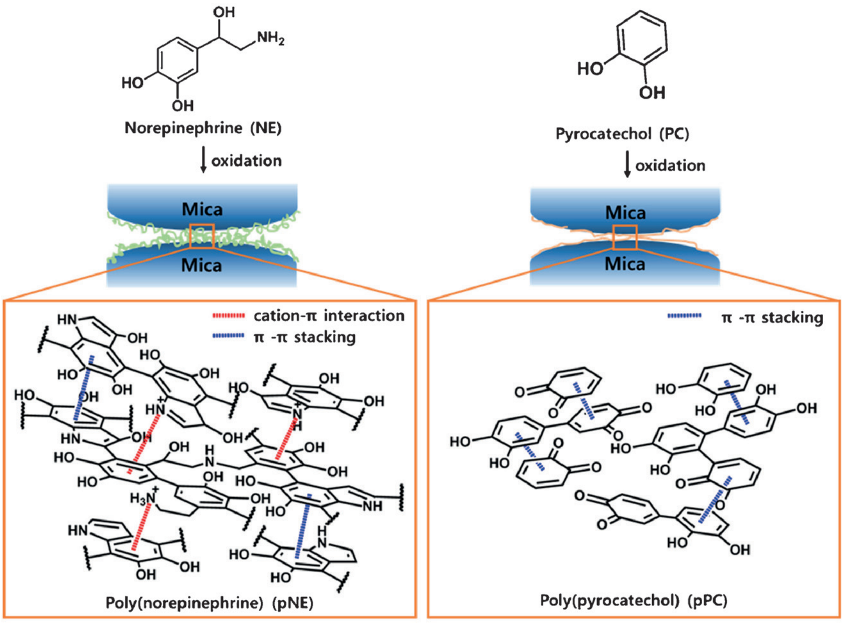

Scheme 1. Chemical structure and schematic representation of surface forces measurements of pNE and pPC using an SFA.

AFM imaging and X-ray photoelectron spectroscopy (XPS) were used to characterize the coated surfaces of pNE and pPC on mica. In Figures 1, and Figures S1, S2, and S3 in the Supporting Information, topographic AFM images show thin layers of both pNE and pPC films coated on mica substrates, and that pNE provides a denser coating than pPC on mica (Figure 1 d). The RMS (root-mean-square) roughness values of the pNE and pPC surfaces were 1.12 nm and 0.44 nm, respectively. It is noted that the pPC film might not fully cover the mica substrate after a relatively short polymerization time. Figure 1 c represents the XPS elemental survey spectrum of mica, and mica coated with pNE and pPC. The strong nitrogen peak of pNE implies that pNE successfully covered the mica surface; however, pPC exhibited a similar survey spectrum to that of mica (no nitrogen peak), which was mainly because pPC did not fully cover the mica during the coating process, as was also confirmed by AFM imaging (Figure 1 b). The coated pNE and pPC surfaces exhibited water contact angles of 30° and 40°, respectively, suggesting successful deposition of the two coatings (Figures 1 and Figure S1). C 1s analysis was also conducted to verify the deposition of the pNE and pPC coatings. The C 1s peaks of pNE and pPC confirm the presence of the coatings on the mica. The higher C 1s peak intensity of pNE compared to pPC shown in Figure 1 d indicates the stronger coating capacity of pNE.

The effect of amine groups on the molecular interactions of pPC and pNE were investigated by using an SFA. Force–distance curves (*F*/*R* vs. *D*) were obtained by coating either pNE or pPC layer on two opposing mica surfaces in 10 mM PBS buffer, at pH 8.4. The "steric wall" distance, that is, the thickness of confined coating materials between two opposing mica surfaces that does not seem to change with an increasing normal compressive load or pressure, was also carefully monitored to probe the time dependence of the thickness of the polycatechol coating on mica. Here, D_{sw} is defined as the D at $F/R \approx 8\ \mathrm{mN\,m^{-1}}$.

By injecting NE or PC that contained a 10 mM PBS buffer at pH 8.4, into the gap between two opposing mica surfaces, in situ polymerization of polycatechols and their coating on both the mica surfaces in the SFA chamber was initiated. The interaction forces between the two polycatechol layers on mica were measured after approximately 30 min. As shown in the representative force–distance profiles in Figures 2 and Figure S4, no significant adhesion ($F_{ad}/R < \approx 1.0\ \mathrm{mN\,m^{-1}}$) was detected in the case of pPC immediately after the in situ polymerization of PC. In contrast, pNE induced strong adhesion ($F_{ad}/R \approx 6.5\ \mathrm{mN\,m^{-1}}$) between the two interacting surfaces immediately after the in situ polymerization of PC. In addition, the adhesion strength gradually increased 220 min after the polymerization initiation and reached up to $F_{ad}/R \approx 30\ \mathrm{mN\,m^{-1}}$ 8 h after the in situ polymerization. It is noted that repetitive adhesion $F_{ad}/R \approx 30\ \mathrm{mN\,m^{-1}}$ could be measured during consecutive force measurements between the two pNE layers 8 h after the in situ polymerization at the same interaction position, and three of such sequential force–distance curves are as shown in Figure S6, which indicates the measured adhesion is reversible. Such reversible adhesion should not be due to irreversible inter-layer covalent cross-linking between pNE surfaces, but caused by some reversible physical interactions (discussed further below).

The adhesive strength between the pNE layers was approximately 30 times higher than that of pPC 8 h after initiating the polymerization process. In addition, the pNE film thickness (i.e., half of the measured steric wall distance)

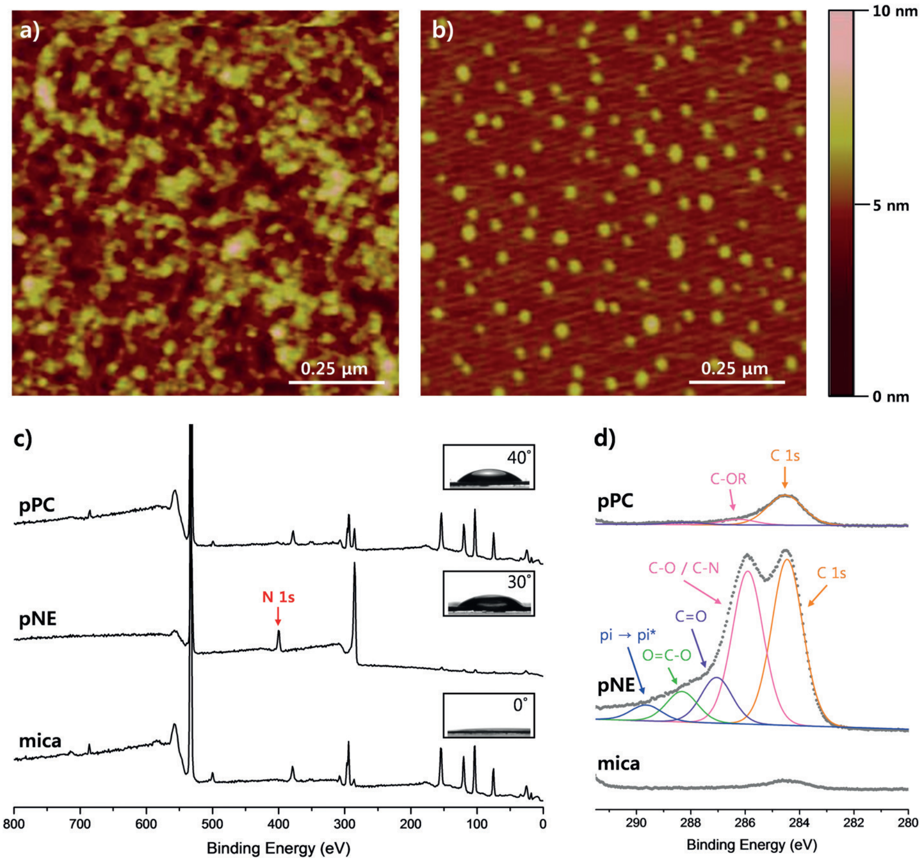

Figure 1. Surface characterization of pNE and pPC coated on mica. AFM image of a) pNE and b) pPC. c) XPS survey of mica, pNE, and pPC (insets: the contact angle of each surface). d) C 1s analysis of each surface.

increased almost 2-fold from 0.8 nm at a polymerization time of $t = 20$ min to 1.6 nm at $t = 480$ min, whereas the thickness of pPC only increased by approximately 35 % over the same polymerization time (Figure 2 c).

The adhesion results for the two pNE coatings and two pPC layers are summarized in Figure 2 b, which shows that the pNE has a much stronger cohesion capacity than pPC. These results imply that amine functional groups can significantly contribute to the adhesion between polyphenol films.

How is the molecular attraction of the poly(catechol) coating enhanced by introducing a primary amine group when poly(catechol) polymerizes in aqueous solutions? Because the zeta potential of a poly(catechol) coating is generally negative,[20] electrostatic attraction can be ruled out. Hydrogen bonds and van der Waals forces could contribute to adhesion but these would not be dominant factors resulting in the strong attraction measured. Instead, the origin of the strong attraction is probably π–π stacking (the quadrupole–quadrupole interaction), cation–π interaction (the monopole–quadrupole interaction), surface salt displacement by the primary amine, and hydrophobic interaction.[21–27]

The oxidative reaction of NE goes through several important intermediate forms, such as 5,6-dihydroxyindole (DHI), 3,4-dihydroxybenzaldehyde (DHBA), and DHBA-NE (product of a Schiff-base formation reaction between DHBA and NE), and finally results in polyindolic crosslinking (Scheme 1, left).[4b,18,28] In contrast, the oxidation of pyrocatechol passes through a quinone intermediate and leads to polyphenolic crosslinking (Scheme 1, right). The difference in the π-electron density of the side aromatic groups in pNE (polyindolic crosslinking) and pPC (polyphenolic crosslinking) could result in different strengths of π–π stacking (the quadrupole–quadrupole interaction).[22] Generally, indolic compounds exhibit a higher π-electron density than phenolic compounds.[23] Therefore, indolic crosslinks in pNE could contribute to the strong attraction via π–π stacking, because pNE has a higher π-electron density than pPC.

Cation–π interaction, which occurs between cations (e.g. Na^+, K^+, NH_3^+) and the π system (e.g. indole, benzene, phenol),[24] could also contribute to the strong attraction between pNE layers. It has been shown via computer simulation and nanomechanical measurements that cation–π interactions (the monopole–quadrupole interactions) are stronger than electrostatic attractions (the monopole—monopole interactions) under certain conditions in aqueous solutions, owing to their low desolvation penalty.[25] In addition, the contribution of the cation–π interaction to mussel underwater adhesion has been measured.[26] Positively charged protonated primary amine groups in NE, protonated imine groups in DHBA-NE, imine groups in DHI could be candidates for the cation donor and the polyindolic crosslinks in the pNE could act as a π group donor.[4b,18,28] Because pKa_1 and pKa_2 of NE are 8.64 and 9.70, respectively,[29] the primary amine group in NE will exist in the protonated form at pH 8.4, at which the experiment was conducted. In addition, the deprotonation pKa of indole is approximately 17, and as most of the resonance structures of indole bear a positive charge on the nitrogen atom,[30] we may infer that quaternary amine exists in pNE. The N 1s XPS peak of pNE at 401.6 eV supports the existence of quaternary amine ($-NH_3^+$ in NE and $=NH^+$ in pNE),[31] as described in Figure S7. In contrast, pPC does not contain the amine groups which could mediate the cation–π interaction. It is known that positively charged primary amine groups and K^+ show similar interaction strengths with π systems, which is stronger than that of Na^+ and Li^+. The SFA results in Figure S8 show that the adhesion between pNE layers decreases from $F_{ad}/R \approx 30\ mN\,m^{-1}$ to $F_{ad}/R \approx 8.5\ mN\,m^{-1}$ (Figure S8 a) and further to almost 0 (Figure S8b) with increasing the K^+ concentration from 0 to 10 and 100 mм, respectively. These SFA results indicate that K^+ ions could compete with and replace the

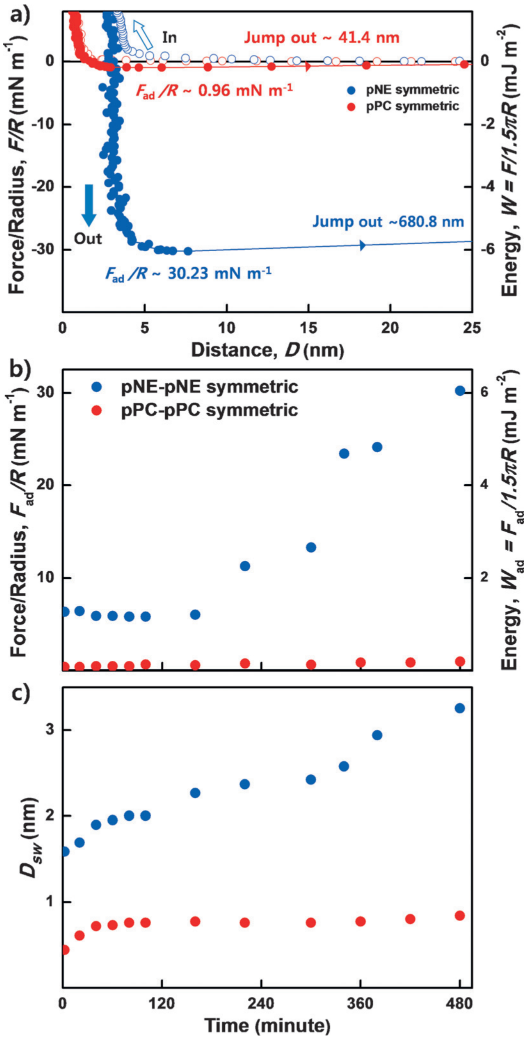

Figure 2. Adhesion energies and thickness of pNE and pPC films as a function of in situ polymerization time at pH 8.4. a) Representative force–distance curves (F/R vs. D) and corresponding interaction energy ($W = F/1.5\pi R$) between two opposing pNE (blue), or pPC (red) layers 8 h after in situ polymerization. Open circle = approach, closed circle = separation. Time dependent b) adhesion and c) film thickness of pNE and pPC films on mica.

positively charged primary amine groups in the cation–π interaction between the two pNE layers, and lead to weakened adhesion.[26]

In addition, it was recently reported that positively charged primary amine groups in mussel adhesive proteins can breach the hydrated salt layer in saline water and assist the catechol in forming a strong bidentate adhesion to inorganic surfaces in wet conditions.[21,32] This synergistic collaboration of catechol and amine groups supports the observed stronger adhesion of a pNE coating compared to that of pPC. Furthermore, DHBA, the intermediate of NE polymerization, exhibited less and also slower auto-oxidation than catechol compounds without an electron-withdrawing group, such as PC.[21]

In summary, this work demonstrates for the first time that the introduction of an amine functional group to the poly(catechol) coating significantly enhances (almost 30-times higher) the adhesion and deposition capability of catechol-based polyphenolic coatings. The origin of the strong attraction between the poly(catecholamine) layers is most likely due to various physical interactions, such as surface salt displacement by the primary amine, π–π stacking (the quadrupole–quadrupole interaction of indolic crosslinks), and cation–π interaction (the monopole–quadrupole interaction between positively charged amine groups and the indolic crosslinks). The results of this study provide insights into the design and development of mussel-inspired catechol-based coating materials.

Experimental Section

pNE, pPC coating for surface characterization: The pNE-coated surface was prepared by immersing mica for 24 h at room temperature in an NE solution, which was prepared by dissolving DL-norepinephrine hydrochloride in 10 mM PBS buffer (pH 8.4) at 2 mg mL^{-1}. The pPC-coated surface was prepared using the same procedure. The coated substrates were washed with deionized water and dried using nitrogen gas. Successful deposition of the pNE and pPC coating was confirmed by X-ray photoelectron spectroscopy (XPS, K-alpha, Thermo VG Scientific, USA) and analysis of the contact angles (SEO, Republic of Korea). The surface morphology of the substrates was measured by atomic force microscope (AFM, Veeco, USA).

Nanomechanical measurement using surface forces apparatus: A SFA (SurForce LLC, Santa Barbara, CA, USA) system was used to measure the nanomechanical properties of polymerized NE and PC in aqueous solutions. Back-silvered muscovite mica surfaces (Grade #1, S&J Trading, Floral Park, NY, USA) were glued onto cylindrical glass disks using an epoxy glue (EPON 1004 F$^{®}$, Exxon Chemicals, Irving, TX, USA) with the thickness of silver to be ca. 50 nm. After that, the two disks were mounted into the SFA chamber in a cross-cylinder configuration. A droplet of ca. 70 µL NE or PC solution was directly injected into the two opposing mica surfaces for polymerization using a syringe, and the SFA chamber was saturated with water vapor. The NE or PC solutions were then prepared using the same method as described in surface characterization part. The film thickness and absolute separation distance were obtained in situ by employing an optical technique named Multiple Beam Interferometry (MBI) using the fringes of equal chromatic order (FECO). The measured force, F, between two curved surfaces, was correlated to the interaction energy per unit area ($W(D)$) of two planar surfaces using the Derjaguin approximation [Eq. (1)].[33]

$$F(D) = 2\pi R W(D) \qquad (1)$$

The interactions between the two pNE layers and two pPC layers were measured at an interval of approximately 30 min at room temperature.

Acknowledgements

This work was supported by the Marine Biotechnology program (Marine BioMaterials Research Center) funded by the Ministry of Oceans and Fisheries, Korea (D11013214H480000110, D.S. Hwang). This work was also supported in part by the National Research Foundation of Korea Grant funded by the Ministry of Science, ICT and Future Planning (MSIP) (NRF-2014R1A2A2A01006724&NRF-C1ABA001-2011-0029960)

and an NSERC Discovery Grant Award and an NSERC RTI Grant Award from the Natural Sciences and Engineering Research Council of Canada (H. Zeng).

Keywords: adhesive strength · catecholamine · cation–π interaction · coatings · π interactions

How to cite: *Angew. Chem. Int. Ed.* **2016**, *55*, 3342–3346
Angew. Chem. **2016**, *128*, 3403–3407

[1] J. H. Waite, M. L. Tanzer, *Science* **1981**, *212*, 1038.

[2] a) B. P. Lee, J. L. Dalsin, P. B. Messersmith, *Biomacromolecules* **2002**, *3*, 1038; b) H. Lee, K. D. Lee, K. B. Pyo, S. Y. Park, H. Lee, *Langmuir* **2010**, *26*, 3790.

[3] a) K. Kim, J. H. Ryu, D. Y. Lee, H. Lee, *Biomater. Sci.* **2013**, *1*, 783; b) J. H. Ryu, S. Jo, M. Y. Koh, H. Lee, *Adv. Funct. Mater.* **2014**, *24*, 7709.

[4] a) C. Lee, J. Shin, J. S. Lee, E. Byun, J. H. Ryu, S. H. Um, D. I. Kim, H. Lee, S. W. Cho, *Biomacromolecules* **2013**, *14*, 2004; b) M. H. Ryou, J. Kim, I. Lee, S. Kim, Y. K. Jeong, S. Hong, J. H. Ryu, T. S. Kim, J. K. Park, H. Lee, J. W. Choi, *Adv. Mater.* **2013**, *25*, 1571.

[5] a) H. Lee, S. M. Dellatore, W. M. Miller, P. B. Messersmith, *Science* **2007**, *318*, 426; b) J. H. Waite, X. X. Qin, *Biochemistry* **2001**, *40*, 2887.

[6] a) J. P. Park, M. J. Choi, S. H. Kim, S. H. Lee, H. Lee, *Appl. Environ. Microbiol.* **2014**, *80*, 43; b) C. Yang, X. Ding, R. J. Ono, H. Lee, L. Y. Hsu, Y. W. Tong, J. Hedrick, Y. Y. Yang, *Adv. Mater.* **2014**, *26*, 7346.

[7] S. H. Ku, J. Ryu, S. K. Hong, H. Lee, C. B. Park, *Biomaterials* **2010**, *31*, 2535.

[8] H. J. Park, K. Yang, M. J. Kim, J. Jang, M. Lee, D. W. Kim, H. Lee, S. W. Cho, *Biomaterials* **2015**, *50*, 127.

[9] J. W. Cui, Y. Yan, G. K. Such, K. Liang, C. J. Ochs, A. Postma, F. Caruso, *Biomacromolecules* **2012**, *13*, 2225.

[10] a) M. H. Ryou, Y. M. Lee, J. K. Park, J. W. Choi, *Adv. Mater.* **2011**, *23*, 3066; b) S. M. Kang, M. H. Ryou, J. W. Choi, H. Lee, *Chem. Mater.* **2012**, *24*, 3481.

[11] B. G. Kim, S. Kim, H. Lee, J. W. Choi, *Chem. Mater.* **2014**, *26*, 4757.

[12] J. S. Kim, T. H. Hwang, B. G. Kim, J. Min, J. W. Choi, *Adv. Funct. Mater.* **2014**, *24*, 5359.

[13] I. You, S. M. Kang, S. Lee, Y. O. Cho, J. B. Kim, S. B. Lee, Y. S. Nam, H. Lee, *Angew. Chem. Int. Ed.* **2012**, *51*, 6126; *Angew. Chem.* **2012**, *124*, 6230.

[14] H. Lee, N. F. Scherer, P. B. Messersmith, *Proc. Natl. Acad. Sci. USA* **2006**, *103*, 12999.

[15] Q. Y. Lu, E. Danner, J. H. Waite, J. N. Israelachvili, H. B. Zeng, D. S. Hwang, *J. R. Soc. Interface* **2013**, *10*, 20120759.

[16] K. Y. Ju, Y. Lee, S. Lee, S. B. Park, J. K. Lee, *Biomacromolecules* **2011**, *12*, 625.

[17] a) S. Hong, J. Yeom, I. T. Song, S. M. Kang, H. Lee, H. Lee, *Adv. Mater. Interfaces* **2014**, *1*, 1400113; b) S. M. Kang, J. Rho, I. S. Choi, P. B. Messersmith, H. Lee, *J. Am. Chem. Soc.* **2009**, *131*, 13224.

[18] S. Hong, J. Kim, Y. S. Na, J. Park, S. Kim, K. Singha, G. I. Im, D. K. Han, W. J. Kim, H. Lee, *Angew. Chem. Int. Ed.* **2013**, *52*, 9187; *Angew. Chem.* **2013**, *125*, 9357.

[19] a) H. Ejima, J. J. Richardson, K. Liang, J. P. Best, M. P. van Koeverden, G. K. Such, J. Cui, F. Caruso, *Science* **2013**, *341*, 154; b) T. S. Sileika, D. G. Barrett, R. Zhang, K. H. Lau, P. B. Messersmith, *Angew. Chem. Int. Ed.* **2013**, *52*, 10766; *Angew. Chem.* **2013**, *125*, 10966.

[20] H. Xu, X. Liu, G. Su, B. Zhang, D. Wang, *Langmuir* **2012**, *28*, 13060.

[21] G. P. Maier, M. V. Rapp, J. H. Waite, J. N. Israelachvili, A. Butler, *Science* **2015**, *349*, 628.

[22] a) J. H. Williams, *Acc. Chem. Res.* **1993**, *26*, 593; b) S. Mecozzi, A. P. West, D. A. Dougherty, *Proc. Natl. Acad. Sci. USA* **1996**, *93*, 10566.

[23] a) D. A. Dougherty, *Science* **1996**, *271*, 163; b) J. P. Gallivan, D. A. Dougherty, *Proc. Natl. Acad. Sci. USA* **1999**, *96*, 9459.

[24] J. C. Ma, D. A. Dougherty, *Chem. Rev.* **1997**, *97*, 1303.

[25] a) Y. Marcus, *Biophys. Chem.* **1994**, *51*, 111; b) J. P. Gallivan, D. A. Dougherty, *J. Am. Chem. Soc.* **2000**, *122*, 870; c) J. S. Rao, H. Zipse, G. N. Sastry, *J. Phys. Chem. B* **2009**, *113*, 7225.

[26] a) Q. Lu, D. X. Oh, Y. Lee, Y. Jho, D. S. Hwang, H. Zeng, *Angew. Chem. Int. Ed.* **2013**, *52*, 3944; *Angew. Chem.* **2013**, *125*, 4036; b) S. Kim, A. Faghihnejad, Y. Lee, Y. Jho, H. Zeng, D. S. Hwang, *J. Mater. Chem. B* **2015**, *3*, 738.

[27] a) P. C. Kearney, L. S. Mizoue, R. A. Kumpf, J. E. Forman, A. McCurdy, D. A. Dougherty, *J. Am. Chem. Soc.* **1993**, *115*, 9907; b) L. M. Salonen, M. Ellermann, F. Diederich, *Angew. Chem. Int. Ed.* **2011**, *50*, 4808; *Angew. Chem.* **2011**, *123*, 4908.

[28] M. d'Ischia, A. Napolitano, A. Pezzella, P. Meredith, T. Sarna, *Angew. Chem. Int. Ed.* **2009**, *48*, 3914; *Angew. Chem.* **2009**, *121*, 3972.

[29] W. M. Haynes in *CRC Handbook of Chemistry and Physics*, 93rd ed., CRC Press, Florida, **2012**, p. 5.

[30] W. J. Houlihan, *The chemistry of Heterocyclic compounds: Indoles*, Wiley, Hoboken, **2009**, pp. 55–56.

[31] a) H. M. Jeong, J. W. Lee, W. H. Shin, Y. J. Choi, H. J. Shin, J. K. Kang, J. W. Choi, *Nano Lett.* **2011**, *11*, 2472; b) S. Bourbigot, M. L. Bras, L. Gengembre, R. Delobel, *Appl. Surf. Sci.* **1994**, *81*, 299.

[32] a) W. Stumm, J. J. Morgan, *Aquatic Chemistry: Chemical Equilibria and Rates in Natural Waters*, 3rd ed., Wiley, New York, **1996**; b) Y. Akdogan, W. Wei, K. Y. Huang, Y. Kageyama, E. W. Danner, D. R. Miller, N. R. M. Rodriguez, J. H. Waite, S. Han, *Angew. Chem. Int. Ed.* **2014**, *53*, 11253–11256; *Angew. Chem.* **2014**, *126*, 11435–11438.

[33] J. N. Israelachvili, *Intermolecular and Surface Forces*, Revised 3rd ed., Academic press, San Diego, **2011**.

Received: November 6, 2015
Published online: February 2, 2016